

ChemComm

Accepted Manuscript



This is an *Accepted Manuscript*, which has been through the Royal Society of Chemistry peer review process and has been accepted for publication.

Accepted Manuscripts are published online shortly after acceptance, before technical editing, formatting and proof reading. Using this free service, authors can make their results available to the community, in citable form, before we publish the edited article. We will replace this *Accepted Manuscript* with the edited and formatted *Advance Article* as soon as it is available.

You can find more information about *Accepted Manuscripts* in the [Information for Authors](#).

Please note that technical editing may introduce minor changes to the text and/or graphics, which may alter content. The journal's standard [Terms & Conditions](#) and the [Ethical guidelines](#) still apply. In no event shall the Royal Society of Chemistry be held responsible for any errors or omissions in this *Accepted Manuscript* or any consequences arising from the use of any information it contains.



www.rsc.org/chemcomm

Cite this: DOI: 10.1039/c0xx00000x

www.rsc.org/xxxxxx

COMMUNICATION

Multimodal luminescent-magnetic boron nitride nanotubes @ NaGdF₄: Eu structures for cancer therapyXia Li,^{*a} Nobutaka Hanagata,^b Xuebin Wang,^a Maho Yamaguchi,^a Wei Yi,^a Yoshio Bando^a and Dmitri Golberg^{*a}

Received (in XXX, XXX) Xth XXXXXXXXXX 20XX, Accepted Xth XXXXXXXXXX 20XX

DOI: 10.1039/b000000x

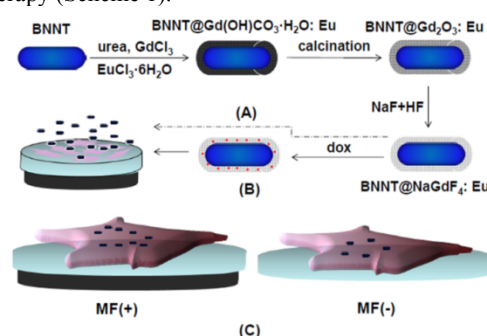
Boron nitride nanotubes@NaGdF₄:Eu composites with core@shell structures were fabricated giving the opportunity to trace, target and thus to manipulate BNNTs in vitro. The composites show the significantly higher cellular uptake and chemotherapy drug intracellular delivery ability in the presence of an external magnetic field than that in its absence.

Boron nitride nanotubes (BNNTs)¹, as a structural analogue of carbon nanotubes (CNTs), have recently attracted increasing attentions in the biomedical field, e.g. with respect to drug delivery^{2, 3}, boron neutron capture cancer therapy⁴, irreversible lethal electroporation cancer treatment⁵, etc. Overall, multi-walled BNNTs show better biocompatibility than CNTs⁶. The exploration of BNNTs for cancer therapy is a promising direction. Boron neutron capture therapy (BNCT) is a targeted radiation therapy for cancer that significantly increases the therapeutic ratio relative to conventional radiotherapeutic modalities⁷. Boron-containing nanoparticles, such as BN nanotubes⁴, boron carbide⁸ and C₂B₁₀ carborane cages attached CNTs⁹ have shown high concentration of boron atoms in tumor cells than in blood and other organs, which provided the delivery of boron to tumor cells for an effective boron neutron capture for cancer therapy. On the other hand, the exploration of BNNTs as an anticancer drug delivery system could provide an integrated vector system³ by combining chemotherapy with other cancer therapy methods. Up to now, the exploration of multifunctional BNNTs for cancer therapy is rarely reported.

A major goal in nanomedicine is the coherent implementation of multifunctional platforms within a single targeted nanodelivery system that would simultaneously perform diagnosis, imaging, targeted delivery and efficient therapy^{10, 11}. Recently, the lanthanide - doped sodium gadolinium fluoride (NaGdF₄:Ln) has been realized to be a promising multimodal bioprobe with photoluminescent imaging and magnetic targeting properties^{11, 12}. Thus, the fabrication of BNNTs@ europium doped sodium gadolinium fluoride (NaGdF₄:Eu) core@shell nanostructures with both fluorescence imaging and magnetic targeting properties will

provide a support for BNNTs in biomedical applications, especially for cancer therapy.

Herein, we realize the functionalization of BNNTs with NaGdF₄: Eu by using urea which acts as the precipitation agents and using the subsequent treatment (Scheme 1). The BNNTs@NaGdF₄: Eu composite emits visible luminescence upon excitation and can be manipulated using an external magnetic field¹³ for the enhanced cellular uptake during cancer imaging and therapy (Scheme 1).



Scheme 1. (A) Synthesis of a BNNTs@NaGdF₄:Eu composite for fluorescence tracing and magnetic targeted particles endocytosis; (B) Magnetic targeted chemotherapy drug delivery of a BNNTs@NaGdF₄:Eu composite; (C) Different particle endocytosis and dox intracellular delivery in the presence (MF(+)) and absence (MF(-)) of external magnetic field.

The as-prepared BNNTs synthesized by chemical vapour deposition (CVD) were oxidized in air at 1000 °C for 5 h and sonicated in water to obtain the shorten BNNTs, around 1 μm long (Figure. 1a, S1). By carefully controlling the synthesis conditions, the BNNTs were then coated with a layer of amorphous Gd(OH)CO₃·3H₂O: Eu around 20~30 degree in the XRD patterns via a homogeneous precipitation method from an aqueous solution of gadolinium nitrate and urea at 90 °C for 2 h (Figure. 1b). Thermal treatment at 700 °C for 8 h transformed the amorphous Gd(OH)CO₃·3H₂O: Eu into the cubic phase of Gd₂O₃ (Figure. 1c). Afterwards, BNNTs@Gd₂O₃: Eu prepared as the above was reacted with NaF and a HF aqueous solution at 80 °C for 2 h to convert it into BNNTs@NaGdF₄: Eu (Figure. 1d). TEM images (Figures. 2, A,C,D) show the successful fabrication of BN@Gd(OH)CO₃·3H₂O: Eu core@shell structure. And after the series of subsequent treatments, such as thermal treatment or fluoride treatment, BNNTs@Gd₂O₃: Eu and BNNTs@NaGdF₄: Eu still retain the initial core@shell structures, as shown in SEM and TEM images (Figures. 2, B, E, F). Moreover, the thickness of

^a World Premier International Center for Materials Nanoarchitectonics (WPI-MANA), National Institute for Materials Science (NIMS), Namiki 1-1, Tsukuba, Ibaraki 305-0044, Japan.

Email: Golberg.Dmitri@nims.go.jp ; LI.Xia@nims.go.jp;

^b Nanotechnology Innovation Station, National Institute for Materials Science (NIMS), 1-2-1 Sengen, Tsukuba, 305-0047, Japan.

†Electronic Supplementary Information (ESI) available: See

DOI: 10.1039/b000000x/

shell can be adjusted from 20nm to 80nm when the initial gadolinium precursor GdCl_3 amounts increase from low to high.

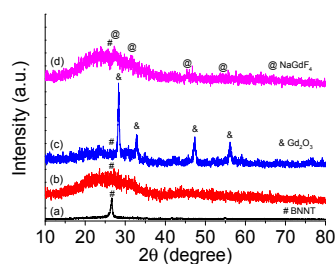


Fig. 1 XRD patterns of BNNTs (a), BNNTs@ $\text{Gd}(\text{OH})\text{CO}_3 \cdot \text{H}_2\text{O}:\text{Eu}$ (b), BNNTs@ $\text{Gd}_2\text{O}_3:\text{Eu}$ (c) and BNNTs@ $\text{NaGdF}_4:\text{Eu}$ (d).

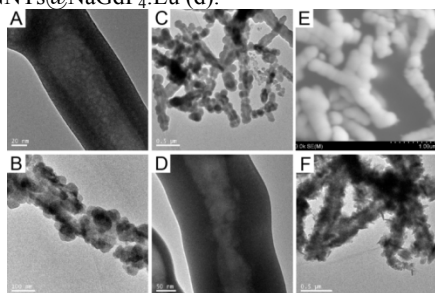


Fig. 2 TEM images of BNNTs@ $\text{Gd}(\text{OH})\text{CO}_3 \cdot \text{H}_2\text{O}:\text{Eu}$ (A) and BNNTs@ $\text{NaGdF}_4:\text{Eu}$ (B) at low GdCl_3 concentration; TEM images of BNNTs@ $\text{Gd}(\text{OH})\text{CO}_3 \cdot \text{H}_2\text{O}:\text{Eu}$ (C,D); SEM image of BNNTs@ $\text{Gd}_2\text{O}_3:\text{Eu}$ (E); TEM image of BNNTs@ $\text{NaGdF}_4:\text{Eu}$ (F) at high GdCl_3 concentration.

Urea is a critical factor for the synthesis of $\text{Gd}(\text{OH})\text{CO}_3 \cdot 3\text{H}_2\text{O}:\text{Eu}$ layer on the surface of BNNTs. Urea acts as the dispersing agent of BNNTs, the precipitation agent and the linking reagent between BNNTs surface and the newly formed $\text{Gd}(\text{OH})\text{CO}_3 \cdot 3\text{H}_2\text{O}:\text{Eu}$. The urea interacted strongly with BNNTs in solution via Van der Waals forces and was adsorbed onto their outer surfaces. This gave a high local concentration of urea on the surface of BNNTs compared to the bulk solution, which bases on the same mechanism as for CNTs¹⁴. For example, much stronger dispersion interaction energy of urea than water with CNTs results in an enhanced urea accumulation in the CNT interior and on the CNT surface¹⁴. After gadolinium nitrate had been added into the above solution, it precipitated on the BNNT surface with the help of local urea. Urea concentration is an important factor to successfully fabricate the core@shell structure. At too low urea concentration, the local concentration of urea on the surface of BNNTs is not high enough to linking BNNTs surface with the newly formed $\text{Gd}(\text{OH})\text{CO}_3 \cdot 3\text{H}_2\text{O}:\text{Eu}$, and then $\text{Gd}(\text{OH})\text{CO}_3 \cdot 3\text{H}_2\text{O}:\text{Eu}$ precipitated separately from BNNTs (Figures. S2, A, B). While, at too high urea concentration, the urea content in the bulk solution is too high. This results in the simultaneous precipitation of $\text{Gd}(\text{OH})\text{CO}_3 \cdot 3\text{H}_2\text{O}:\text{Eu}$ on the BNNTs surface and the formation of discrete $\text{Gd}(\text{OH})\text{CO}_3 \cdot 3\text{H}_2\text{O}:\text{Eu}$ spheres in the bulk solution (Figures. S2, C).

The obtained BNNTs@ $\text{NaGdF}_4:\text{Eu}$ composites exhibit simultaneous fluorescent and magnetic properties. To demonstrate the performance and multicolor emissions of the core@shell structure, photoluminescence emission spectra of BNNTs@ $\text{NaGdF}_4:\text{Eu}$ emitters were measured at room temperature (Figure. 3D). Upon excitation at 325 nm, intense and distinct emission patterns of Eu^{3+} centered at 593 nm and 613 nm were detected in the visible light range. These emission lines can

be explicitly assigned to the transitions of ${}^5\text{D}_0 \rightarrow {}^7\text{F}_1$ and ${}^5\text{D}_0 \rightarrow {}^7\text{F}_2$ for Eu^{3+} , respectively, and thus resulted in red color outputs. The red color emissions of BNNTs@ $\text{NaGdF}_4:\text{Eu}$ composites uptaken by LNCap prostate cancer cells were directly observed by confocal fluorescence microscopy (Figures. 3A,B,C). Field-dependent magnetization curve at room temperature for BNNTs@ $\text{NaGdF}_4:\text{Eu}$ core@shell nanostructure was recorded using a superconducting quantum interference device (SQUID) magnetometer with fields (Figure. 3E). Near-zero coercivity and remanence indicate the superparamagnetic behavior of the composites.

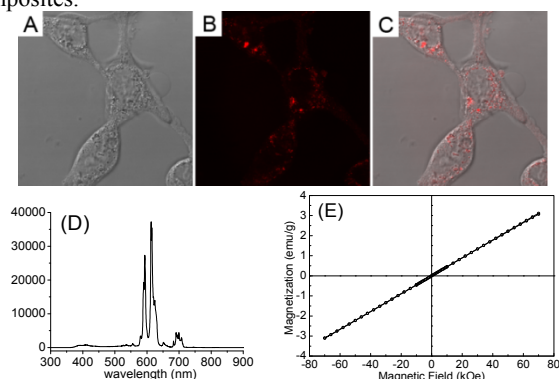


Fig. 3 The differential interference contrast (DIC) image (A), confocal fluorescence image (B) and overlapped (C) image of BNNTs@ $\text{NaGdF}_4:\text{Eu}$ composites endocytosized by LNCap prostate cancer cells; Photoluminescence (PL) emission spectrum upon excitation at 325 nm of the BNNTs@ $\text{NaGdF}_4:\text{Eu}$ composites (D); Room temperature magnetization as a function of magnetic field for a BNNTs@ $\text{NaGdF}_4:\text{Eu}$ composite (E).

In order to demonstrate the utility of BNNTs@ $\text{NaGdF}_4:\text{Eu}$ composites as a targeted cancer therapeutic for BNCT, the effect of magnetic targeting on in vitro cellular uptake using analysis of cell-associated BNNTs@ $\text{NaGdF}_4:\text{Eu}$ fluorescence was evaluated. When human LNCap prostate cancer cells were incubated with BNNTs@ $\text{NaGdF}_4:\text{Eu}$ particle suspensions under the influence of a permanent magnetic field, the significantly higher cell-associated uptake was observed than in the absence of a magnetic field (Figure. 4A). At 20 $\mu\text{g}/\text{mL}$ of BNNTs@ $\text{NaGdF}_4:\text{Eu}$ particle-containing medium, the fluorescence intensity for pure cells, particles-uptaking cells in the absence of a magnetic field and particles-uptaking cells in the presence of a magnetic field was 230 ± 3 , 315 ± 18 and 404 ± 30 , respectively. The cellular uptake in the presence of a magnetic field is increased about 2 times compared with that in its absence.

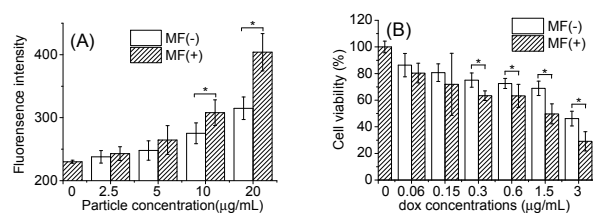


Fig. 4 Fluorescence intensity of BNNTs@ $\text{NaGdF}_4:\text{Eu}$ uptaken by LNCap prostate cancer cells under excitation at 380 nm and emission at 610 nm after 3 hours in the absence (-) and presence (+) of the external magnetic field ($n=4$, $p<0.05$) (A); LNCap prostate cancer cells viability when coculturing with dox-loaded BNNTs@ $\text{NaGdF}_4:\text{Eu}$ in the absence (-) and presence (+) of the external magnetic field for initial 3 hours and subsequent 20 hours when changing the culture medium to original one ($n=6$, $p<0.05$) (B).

To further demonstrate the utility of BNNTs@NaGdF₄: Eu composites as a targeted cancer therapeutic for chemotherapy drug delivery, BNNTs@NaGdF₄: Eu composites were used to load doxorubicin for the investigation of the cancer cells killing ability in the absence and presence of a magnetic field. BNNTs@NaGdF₄: Eu composite shows a loading efficiency of doxorubicin about 30% when pH was 8.0 (Figure. S3). The human LNCap prostate cancer cells viability of the dox-loaded BNNTs@NaGdF₄: Eu composite was studied in the absence and presence of a magnetic field (Figure. 4B). For human LNCap prostate cancer cells, in the absence of a magnetic field, the IC50 value of the initial dox loading amounts for the dox-loaded BNNTs@NaGdF₄: Eu composite was 3 μg mL⁻¹. This value was reduced to 1.5 μg mL⁻¹ in the presence of magnetic field. The decrease in the value of IC50 resulted from the action of the magnetic field guiding, which resulted in the enhanced cellular uptake of the dox-loaded BNNTs@NaGdF₄: Eu composite and thus increased intracellular delivery of dox. The nanostructured composites were well suspended in the cell culture medium, while the LNCap prostate cancer cells attached to the bottom of the plate. The nanostructured composites particles suffer from the downward force towards the magnet beneath the culture plate, which results in the relatively high local concentration on the cancer cells and thus high cellular uptake in the presence of magnet, compared with that in the absence of magnet.

BNNTs@NaGdF₄: Eu composite is a promising agent for simultaneous targeted radiation therapy and chemotherapy. The goal of boron neutron capture therapy is to achieve a high concentration of boron in the tumour while avoiding its accumulation in the normal tissues. However, obtaining sufficient amounts of boron in the tumour tissue by systemic administration of soluble B compounds has been proved to be difficult¹⁵. As an alternative to soluble boron, the possibility that B nanoparticles might hold promise as future therapeutic agents was investigated. Doxorubicin is a broad-spectrum antitumor drug widely used for the treatment of several kinds of cancers, including prostate, breast and ovarian ones. The systemic applications of doxorubicin often cause severe side effects in other tissues, such as cardiomyopathy¹⁶. In addition, rapid elimination and widespread distribution into non-targeted organs and tissues lead to low bioavailability and require the administration of a drug in large quantities, which is not economical. In this study, BNNTs@NaGdF₄: Eu composite shows enhanced human LNCap prostate cancer cells killing ability of the doxorubicin-loaded in the presence of an external magnetic field compared with that in its absence. Thus, BNNTs@NaGdF₄: Eu composite may realize the targeted release of chemotherapy drug under the guiding of an external magnetic field near the tumor sites¹³ to further increase its accumulation in the tumor and decrease its systemic toxicity.

In conclusion, BNNTs@NaGdF₄: Eu core@shell structures are fabricated by using urea as the dispersing agents of BNNTs, the precipitation agents and the linking reagents between BNNTs and NaGdF₄: Eu. The material emits visible luminescence upon excitation and can be directed by an external magnetic field to a specific target, making it an attractive system for a variety of biological applications. Under the influence of an external magnetic field, the significantly higher cell-associated uptake of BNNTs@NaGdF₄: Eu particle by human LNCap prostate cancer cells was observed than in the absence of a magnetic field. Moreover, the multifunctional BNNTs@NaGdF₄: Eu composites show advantages for in vitro enhancement of chemotherapy efficacy by using magnetic fields.

Acknowledgment

The authors are grateful to Drs. X.L. Li, R. Nagano, K. Iiyama and N. Kawamoto for their generous technical assistance. This work was funded by the World Premier International Center for Materials Nanoarchitectonics (WPI-MANA) of the National Institute for Materials Science (NIMS), Tsukuba, Japan.

Notes and references

- 1 D. Golberg, Y. Bando, Y. Huang, T. Terao, M. Mitome, C. C. Tang and C. Y. Zhi, *Acs Nano*, 2010, **4**, 2979-2993.
- 2 G. Ciofani, S. Danti, G. G. Genchi, B. Mazzolai and V. Mattoli, *Small*, 2013, **9**, 1672-1685.
- 3 X. Li, C. Zhi, N. Hanagata, M. Yamaguchi, Y. Bando and D. Golberg, *Chem. Commun.*, 2013, **49**, 7337-7339.
- 4 D. A. Buzatu, J. G. Wilkes, D. Miller, J. A. Darsey, T. Heinze, A. Biris, R. Berger and M. Diggs, *US Pat.*, 7608240., 2009.
- 5 V. Raffa, C. Riggio, M. W. Smith, K. C. Jordan, W. Cao and A. Cuschieri, *Technol. Cancer. Res. Treat.*, 2012, **11**, 459-465.
- 6 X. Chen, P. Wu, M. Rousseas, D. Okawa, Z. Gartner, A. Zettl and C. R. Bertozzi, *J. Am. Chem. Soc.*, 2009, **131**, 890-891; G. Ciofani, S. Danti, D. D'Alessandro, L. Ricotti, S. Moscato, G. Bertoni, A. Falqui, S. Berrettini, M. Petrini, V. Mattoli and A. Menciacsi, *Acs Nano*, 2010, **4**, 6267-6277; D. Lahiri, F. Rouzaud, T. Richard, A. K. Keshri, S. R. Bakshi, L. Kos and A. Agarwal, *Acta. Biomater.*, 2010, **6**, 3524-3533.
- 7 J. A. Coderre and G. M. Morris, *Radiat. Res.*, 1999, **151**, 1-18.
- 8 M. S. Petersen, C. C. Petersen, R. Agger, M. Suttmuller, M. R. Jensen, P. G. Sorensen, M. W. Mortensen, T. Hansen, T. Bjornholm, H. J. Gundersen, R. Huiskamp and M. Hokland, *Anticancer. Res.*, 2008, **28**, 571-576.
- 9 Z. Yinghuai, A. T. Peng, K. Carpenter, J. A. Maguire, N. S. Hosmane and M. Takagaki, *J. Am. Chem. Soc.*, 2005, **127**, 9875-9880.
- 10 Q. Ju, D. T. Tu, Y. S. Liu, R. F. Li, H. M. Zhu, J. C. Chen, Z. Chen, M. D. Huang and X. Y. Chen, *J. Am. Chem. Soc.*, 2012, **134**, 1323-1330;
- 11 C. E. Ashley, E. C. Carnes, G. K. Phillips, D. Padilla, P. N. Durfee, P. A. Brown, T. N. Hanna, J. Liu, B. Phillips, M. B. Carter, N. J. Carroll, X. Jiang, D. R. Dunphy, C. L. Willman, D. N. Petsev, D. G. Evans, A. N. Parikh, B. Chackerian, W. Wharton, D. S. Peabody and C. J. Brinker, *Nat. Mater.*, 2011, **10**, 389-397; Y. Wang, R. Huang, G. Liang, Z. Zhang, P. Zhang, S. Yu and J. Kong, *Small*, 2013; A. L. Antaris, J. T. Robinson, O. K. Yaghi, G. Hong, S. Diao, R. Luong and H. Dai, *Acs Nano*, 2013, **7**, 3644-3652; S. Chen, C. Hoskins, L. Wang, M. P. MacDonald and P. Andre, *Chem. Commun.*, 2012, **48**, 2501-2503; S. Zhang, Z. Zha, X. Yue, X. Liang and Z. Dai, *Chem. Commun.*, 2013, **49**, 6776-6778.
- 12 L. Zhou, Z. Li, E. Ju, Z. Liu, J. Ren and X. Qu, *Small*, 2013.
- 13 Y. Liu, D. Tu, H. Zhu, R. Li, W. Luo and X. Chen, *Adv. Mater.*, 2010, **22**, 3266-3271; P. Ptacek, H. Schäfer, K. Kömpe and M. Haase, *Adv. Funct. Mater.*, 2007, **17**, 3843-3848.
- 14 H. W. Yang, M. Y. Hua, H. L. Liu, R. Y. Tsai, C. K. Chuang, P. C. Chu, P. Y. Wu, Y. H. Chang, H. C. Chuang, K. J. Yu and S. T. Pang, *Acs Nano*, 2012, **6**, 1795-1805.
- 15 P. Das and R. Zhou, *J. Phys. Chem. B.*, 2010, **114**, 5427-5430.
- 16 K. Hideghety, W. Sauerwein, A. Wittig, C. Gotz, P. Paquis, F. Grochulla, K. Haselsberger, J. Wolbers, R. Moss, R. Huiskamp, H. Fankhauser, M. de Vries and D. Gabel, *J. Neurooncol.*, 2003, **62**, 145-156.
- 17 P. Singal, T. M. Li, D. Kumar, I. Danelisen and N. Iliskovic, *Mol. Cell. Biochem.*, 2000, **207**, 77-86.

